

Supporting Information

Nanoconfinement-Enabled GO Hydrogels via Hummers Method for Real-Time Health Monitoring

Lili Tian^{a*}, Zhiming Yang^{a,b*}, Qin Wang^{a,b*}

a. Ningxia Key Laboratory of Green Catalytic Materials and Technology, College of Chemistry and Chemical Engineering, Ningxia Normal University, Guyuan 756099, China

b. Key Laboratory of Soil Ecological Health and Microbial Regulation, School of Resources, Environment and Life Sciences, Ningxia Normal University, Guyuan, 756009, China

*. Corresponding authors.

E-mail addresses: tianlili@nxnu.edu.cn

This PDF includes the experimental section, supplementary Fig S1-S5.

4. Experimental section

4.1 Materials

Acrylamide (AM): Purity $\geq 99\%$, CAS 79-06-1; purchased from Aladdin Biochemical Technology Co., Ltd. (Shanghai, China). (3-Acrylamidophenyl) boronic acid (AAPBA): Purity $\geq 97\%$, CAS 99349-68-5; purchased from Aladdin (Shanghai, China). GO: Improvised; PVA (1799): Degree of polymerization 1700, MW ~ 78000 -82000 g/mol, hydrolysis degree 98~99%, CAS 9002-89-5[7]; MBA: Purity $\geq 99\%$, CAS 110-26-9[10]; all purchased from Aladdin (Shanghai, China).

4.3 Characterization methods

Fourier-transform infrared (FTIR) was performed using a Vertex70 (Bruker, Germany) in the range of 4000–500 cm^{-1} . The morphologies of the freeze-dried elastomer were characterized by scanning electron microscopy (SEM) using a Quanta 450FEG-SEM (FEI, USA). X-ray diffraction (XRD, Bruker D2 Phaser, Germany) patterns were performed under Cu $K\alpha$ radiation ($\lambda = 1.54 \text{ \AA}$).

4.4 Mechanical Tests

The mechanical performance of the elastomer was characterized using a TA.XTC-18 mass tester (Shanghai BaoSheng, China). Column hydrogel specimens with a length of 20.0 mm and diameter of 6.0 mm were used for the tensile tests, and the extension rate was set to 50 mm/min. The cyclic compression performance of the elastomer was characterized using cylindrical specimens (diameter: 6 mm; height: 10 mm) with a constant compression rate of 5 mm/min at room temperature. The time interval between cycles was set to 60 seconds. The tensile stress σ_t was calculated as follows: $\sigma_t = F_t / \pi r^2$, (F_t is the tensile force at strain t of cylindrical hydrogel sample (N), and r is the original radius of the specimen (mm)). The tensile strain ε_R is defined as the change in the grip separation relative to the initial length, $\varepsilon_R = [L_R - L_0 / L_0] \times 100\%$ (L_R is the grip displacement during testing, and L_0 is the length of the sample before tests). The tensile fracture stress or tensile strength (σ_b) and the tensile fracture strain or

elongation at break (ϵ_b) are the tensile stress and strain at which the specimen breaks, respectively.

4.5 Self-healing Tests

The self-healing elastomer was subjected to tensile and compression tests using a TA.XTC-18 mass tester (Shanghai Baosheng, China) to quantify their self-healing efficiency (SE). Cylindrical specimens of elastomer (length = 25.0 mm, diameter = 6.0 mm) were cut into two halves. The cut surfaces were then placed together without applying external pressure to allow self-healing and were carefully sealed to avoid water evaporation from the elastomer. The stretchability of the $A_{35}P_5B_{17.5}M_{15}GO_{1.5}$ was determined after healing for 0.5 h, 1 h, 4h and 6 h.

The stress self-healing efficiency, $SE\sigma = \sigma_s / \sigma_o \times 100\%$, and strain self-healing efficiency, $SE\epsilon = \epsilon_s / \epsilon_o \times 100\%$, were calculated, where σ_s and ϵ_s are the tensile stress and strain of the self-healing specimen, respectively, and σ_o and ϵ_o are the tensile stress and strain of the original specimen without cutting, respectively.

4.6 Rheological Measurements

The rheological behavior of the $A_{35}P_5B_{17.5}M_{15}GO_{1.5}$ was analyzed using a modular compact rheometer (MCR 302; Anton Paar, China). The samples were prepared as round specimens (thickness: 1 mm; diameter: 25 mm). A strain scan test of the $A_{35}P_5B_{17.5}M_{15}GO_{1.5}$ composite hydrogel was performed at strains ranging from 0.1% to 1000% and a frequency of 10 rad/s. Step strain sweep measurements were conducted at a frequency of 10 rad/s, and the strain was changed from 1% to 300% to achieve a strain failure. Self-healing experiments were performed at room temperature unless otherwise stated.

4.7 Electrical and sensing performances

The electrical conductivities of the elastomers were measured using an Autolab electrochemical workstation (Aptar, Switzerland, Europe). The sensing performance of the elastomer for various human activities (e.g., finger, wrist, and knee movements), as well as for throat movements, was characterized by placing the elastomer at appropriate locations.

The relative resistance ($\Delta R / R_0$) was obtained using Equation (1):

$$\Delta R / R_0 = (R - R_0) / R_0 = (I_0 - I) / I \quad (1)$$

where I_0 and I denote the initial and real-time currents, respectively. R and R_0 are the resistances with and without the applied strain, respectively. The strain sensitivity of the hydrogel was evaluated using the gauge factor (GF) and calculated using Equation (2):

$$GF = (R - R_0) / (R_0 \times \varepsilon) \quad (2)$$

where R_0 , R , and ε are the pristine resistance, real-time resistance, and strain, respectively.

The conductivities were assessed using the AC impedance method over the frequency range of 10^{-1} – 10^6 Hz. The conductivity σ ($S\ m^{-1}$) was obtained using Equation (3):

$$\sigma = d/R \times A \quad (3)$$

where d , R , and A are the distance between adjacent electrodes, impedance, and cross-sectional area of the samples, respectively.

The dimensions of the elastomer sensors for all the sensing characterization experiments were approximately 60 mm (length) \times 10 mm (width) \times 2 mm (thickness).

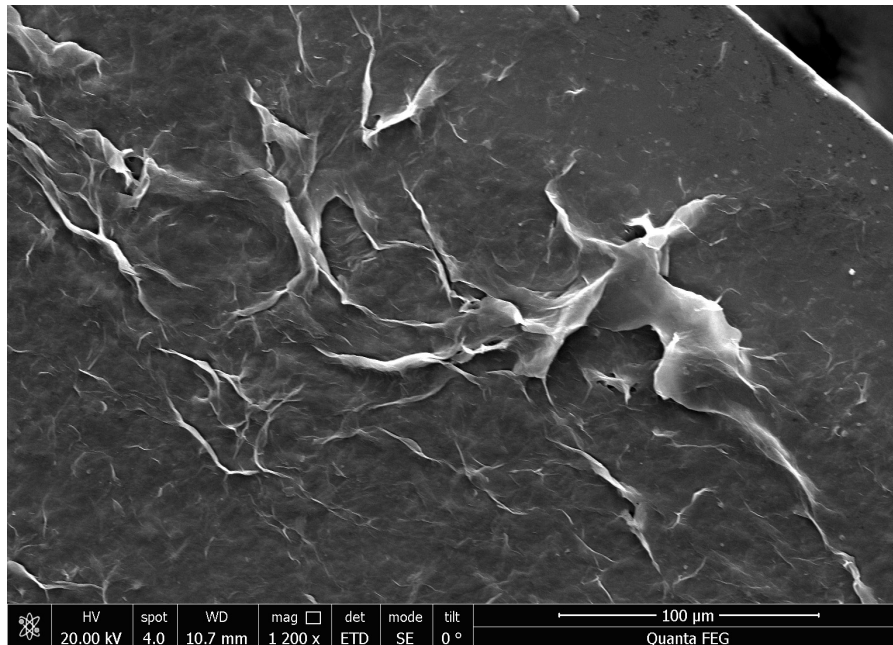


Fig. S1 SEM image of GO

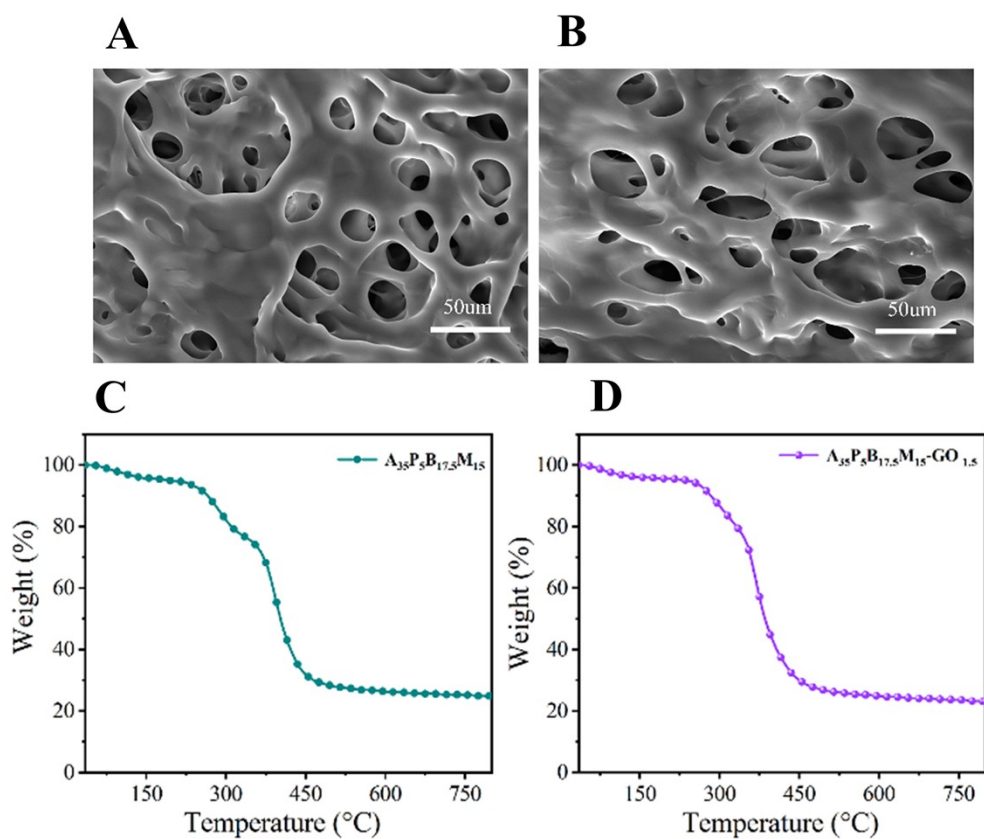


Fig. S2 SEM image of hydrogel cross-section and TGA , (A) (C) $A_{35}P_5B_{17.5}M_{15}$,
(B) (D) $A_{35}P_5B_{17.5}M_{15}GO_{1.5}$

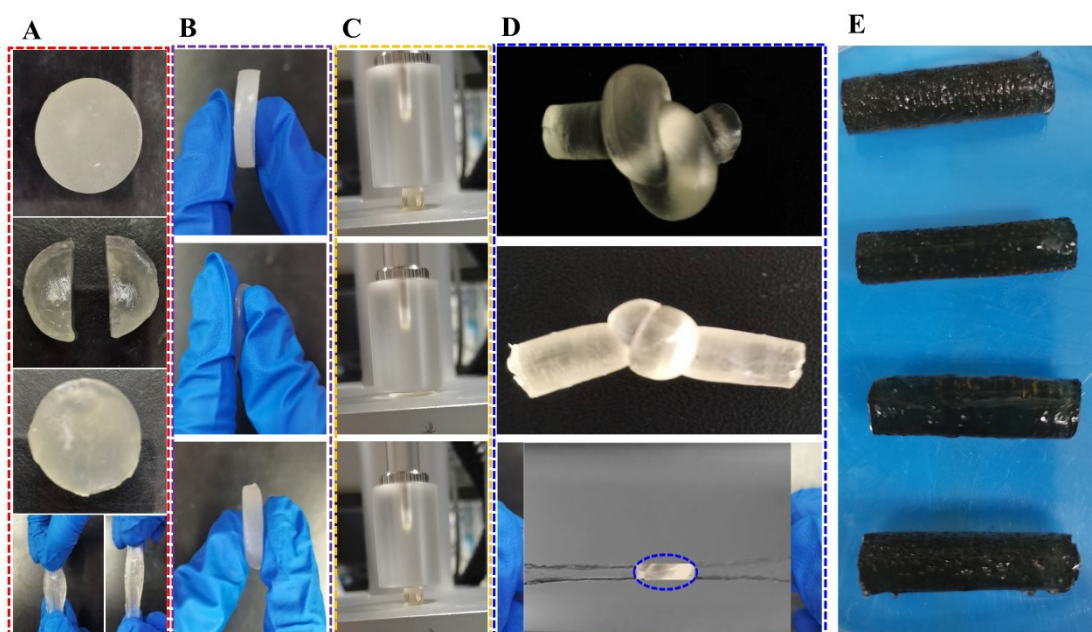


Fig. S3 $A_{35}P_5B_{17.5}M_{15}$ hydrogels show excellent self-healing and recovery under (A)self-healing post-stretching, (B)extrusion, (C)compression and (D)knotting conditions, (E)Digital photographs of hydrogels with different GO contents

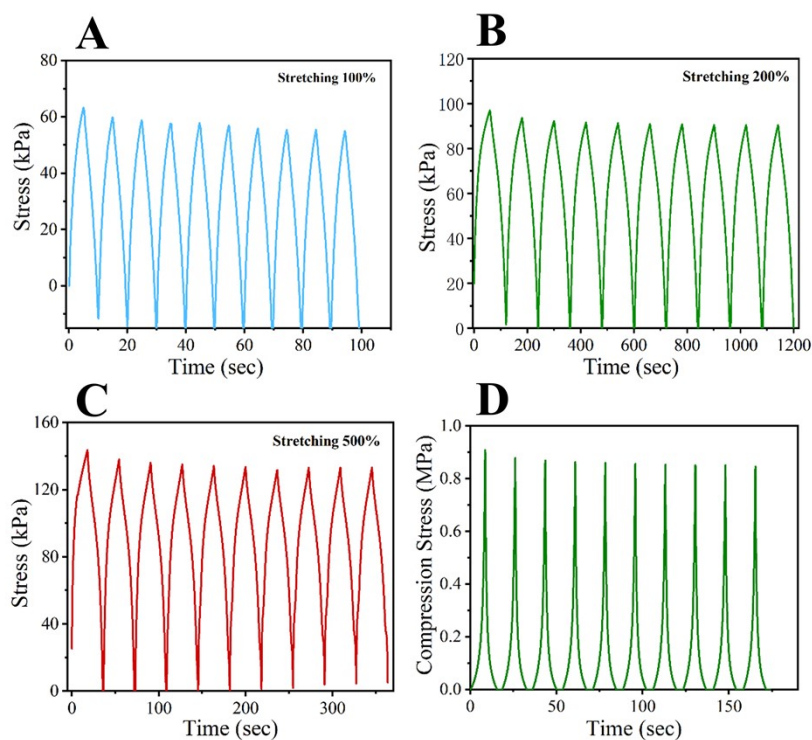


Fig. S4 Cyclic tensile and compression of $A_{35}P_5B_{17.5}M_{15}GO_{1.5}$ at different strains, (10 cycles) (a)100%, (b)200% and (c)500% stress-strain, (d-f) for 100%-500% stress-time plots, (g)90% strain-stress cyclic compression and (h)stress-time

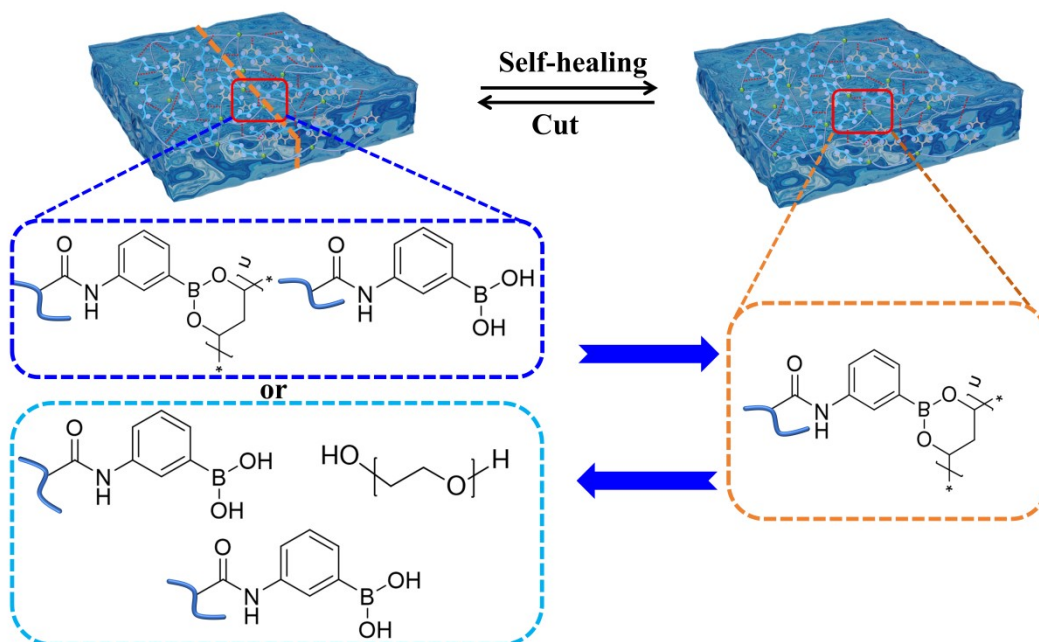


Fig. S5 Self-healing mechanism of hydrogels mediated by dynamic chemical bonds